



drones



Article

How Big Is That Manta Ray? A Novel and Non-Invasive Method for Measuring Reef Manta Rays Using Small Drones

Edy Setyawan, Ben C. Stevenson, Muhamad Izuan, Rochelle Constantine and Mark V. Erdmann

Special Issue

Drones for Biodiversity Conservation

Edited by


Dr. Margarita Mulero-Pazmany and Dr. Barbara Bollard



<https://doi.org/10.3390/drones6030063>

Article

How Big Is That Manta Ray? A Novel and Non-Invasive Method for Measuring Reef Manta Rays Using Small Drones

Edy Setyawan ^{1,*} , Ben C. Stevenson ², Muhamad Izuan ³, Rochelle Constantine ^{1,4} and Mark V. Erdmann ⁵

¹ Institute of Marine Science, The University of Auckland, Auckland 1010, New Zealand; r.constantine@auckland.ac.nz

² Department of Statistics, The University of Auckland, Auckland 1010, New Zealand; ben.stevenson@auckland.ac.nz

³ POKJA Manta, Waisai 98471, Indonesia; izuan07@gmail.com

⁴ School of Biological Sciences, The University of Auckland, Auckland 1010, New Zealand

⁵ Conservation International Aotearoa, The University of Auckland, Auckland 1010, New Zealand; merdmann@conservation.org

* Correspondence: eset230@aucklanduni.ac.nz or edysetyawan@gmail.com

Abstract: This study explores the application of small, commercially available drones to determine morphometric the measurements and record key demographic parameters of reef manta rays (*Mobula alfredi*) in Raja Ampat, Indonesia. DJI Mavic 2 Pro drones were used to obtain videos of surface-feeding *M. alfredi* with a floating, known-length PVC pipe as a reference scale—thus avoiding the need to utilize altitude readings, which are known to be unreliable in small drones, in our photogrammetry approach. Three dimensions (disc length (DL), disc width (DW), and cranial width (CW)) from 86 different individuals were measured. A hierarchical multivariate model was used to estimate the true measurements of these three dimensions and their population-level multivariate distributions. The estimated true measurements of these dimensions were highly accurate and precise, with the measurement of CW more accurate than that of DL and, especially, of DW. Each pairing of these dimensions exhibited strong linear relationships, with estimated correlation coefficients ranging from 0.98–0.99. Given these, our model allows us to accurately calculate DW (as the standard measure of body size for mobulid rays) using the more accurate CW and DL measurements. We estimate that the smallest mature *M. alfredi* of each sex we measured were 274.8 cm (males, $n = 30$) and 323.5 cm DW (females, $n = 8$). We conclude that small drones are useful for providing an accurate “snapshot” of the size distribution of surface-feeding *M. alfredi* aggregations and for determining the sex and maturity of larger individuals, all with minimal impact on this vulnerable species.

Keywords: aerial photogrammetry; marine megafauna; unmanned aerial vehicle; sexual dimorphism; size at maturity



Citation: Setyawan, E.; Stevenson, B.C.; Izuan, M.; Constantine, R.; Erdmann, M.V. How Big Is That Manta Ray? A Novel and Non-Invasive Method for Measuring Reef Manta Rays Using Small Drones. *Drones* **2022**, *6*, 63. <https://doi.org/10.3390/drones6030063>

Academic Editors:
Margarita Mulero-Pazmany and
David R. Green

Received: 31 December 2021

Accepted: 25 February 2022

Published: 28 February 2022

Publisher's Note: MDPI stays neutral with regard to jurisdictional claims in published maps and institutional affiliations.



Copyright: © 2022 by the authors. Licensee MDPI, Basel, Switzerland. This article is an open access article distributed under the terms and conditions of the Creative Commons Attribution (CC BY) license (<https://creativecommons.org/licenses/by/4.0/>).

1. Introduction

Body size is a life-history parameter used to provide insights into key aspects of species and individual biology, including the maturity stage, reproductive status, population demographics, and environmental and habitat conditions to which individuals are exposed [1–4]. Therefore, obtaining accurate measurements of animal body size is crucial for the conservation and management of most animal species [2]. Measuring the morphometric features of large animals, which can be difficult or dangerous to approach, can be problematic [3,5]. Most methods require close contact with or restraint of the animals, which has the potential to impact negatively upon them [6]. Photogrammetry, a non-invasive approach, allows us to accurately obtain measurements of large animals without physical contact [2,7]. Photogrammetry has been used to estimate the length, body weight, and other size measurements of a wide variety of animal species, from sheep to sharks to dolphins [8–10].

The reef manta ray (*Mobula alfredi*) is listed as vulnerable on the IUCN Red List of Threatened Species, primarily due to fisheries' exploitation (both as a target and as bycatch) of this slow-breeding species [11]. Comprehensive information on the body size and size at maturity of manta rays is important to understand their life history and to design effective conservation management strategies [12,13]. To date, three methods have been commonly used to measure the body size of free-swimming manta rays, including visual estimation [12], paired laser photogrammetry [5], and estimation using paired stereo-video camera systems [14].

Of these three techniques, underwater visual estimation is the most commonly-used method to record the size of *M. alfredi*; typically, disc width (DW, defined by Notarbartolo Di Sciara [15] as the greatest dimension between the outermost tips of the pectoral fins) is estimated based on the lengths obtained by divers or snorkelers directly above, below, or next to manta rays [12,16]. Despite the ease and practicality of this approach, visual size estimation can generate significant biases and inconsistencies in size estimates [17].

In an attempt to improve upon the accuracy of the visual estimation approach, Deakos [5] and Couturier et al. [18] utilized paired laser photogrammetry to measure the body size of *M. alfredi* in Hawaii and eastern Australia, respectively. Two laser pointers were mounted parallel to each other on an aluminum plate and at a measured distance apart from one another, with a video or still camera mounted midway between the two pointers. The laser pointers projected two light points, which were a known distance apart (either 50 cm [18] or 60 cm [5]), onto the manta ray, thereby allowing the extrapolation of the manta ray's size using readily available photo-processing software [5].

More recently, a paired stereo-video camera system has been used to measure *M. alfredi* in the Seychelles [14]. This technique utilizes a pair of video cameras mounted on a bar at a measured distance apart, allowing the overlap of the cameras' field of view [19]. The resulting paired images of each manta ray are processed with custom software that allows the calculation of the size of the animal; this technique has been proven to estimate the length of fishes more accurately than the visual estimation technique [20], and has recently been used to accurately measure whale sharks, *Rhincodon typus* [17], and oceanic whitetip reef sharks, *Carcharhinus longimanus* [21]. While the aforementioned methods have been used with increasing accuracy to measure the body size of *M. alfredi*, all three methods require a diver or snorkeler to be in the water with the manta rays to visually estimate their size or operate the camera setups, which can be time-consuming and costly and can potentially lead to negative behavioral responses from the manta rays being measured [22].

Importantly, many authors attempting to measure the body size of manta rays have expressed concern over the use of the disc width (DW) dimension, noting that it can be difficult to reliably measure the maximum distance between the fully-extended wing tips for a variety of reasons—ranging from the challenge of photographing free-swimming manta rays at exactly the moment of maximum extension of the pectoral fins [5,23,24] to issues with preserved specimens that have been stored with the wings in a curled fashion, which prevents straight-line measurement [15]. Nonetheless, DW remains the standard measure of body size for all rays in the order Myliobatiformes, including manta rays in the family Mobulidae [25]. Because of the fragility and common breakage of the elongated tails, measures of total or standard length (TL or SL) common for most other fishes are considered unreliable in these rays, with DW being the largest reliably measurable dimension [15]. Because of the difficulties of measuring DW in live manta rays especially, previous authors have suggested measuring disc length (DL, defined by Notarbartolo Di Sciara [15] as the dimension measured from the midpoint of the rostral margin to the free rear tip of the pectoral fin; Figure 1) as a more easily and accurately measurable dimension of size, from which DW can then be readily calculated using a regression formula (e.g., Deakos [5]).

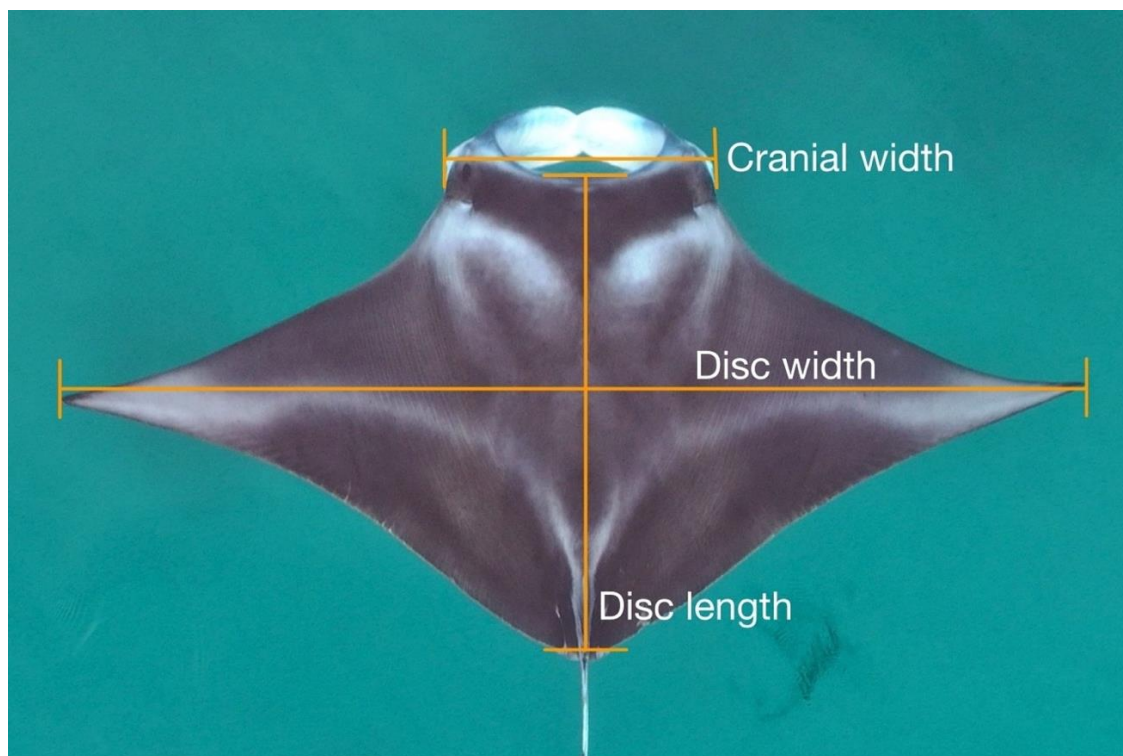


Figure 1. Three dimensions (disc width—DW, disc length—DL, and cranial width—CW) of *M. alfredi* measured during image processing, as defined by Notarbartolo Di Sciara [15].

Drones are an emerging technology that are increasingly affordable and easy to operate and have been used extensively for a wide variety of marine research purposes [26–30]. We believe drones have tremendous potential to address some of the difficulties involved in measuring body size in manta rays with little or no disruptive interaction with the observed animals. The measurements generated using drones through photogrammetry, however, are imperfect and subject to errors and uncertainties, resulting from various factors, including in altitude reading, image quality, and the position of objects in the water [31–33]. Given these concerns, statistical methods for analyzing drone-based measurements are required to assess these errors if they are non-negligible [34].

Taking the above into account, we report here the development of a novel method using small, commercially available drones to measure the body size of surface-feeding *M. alfredi* in Raja Ampat, West Papua, Indonesia. Specifically, we employed aerial photogrammetry techniques, including a floating polyvinyl chloride (PVC) pipe of known length as a reference scale, to measure three morphometric dimensions of *M. alfredi*: the aforementioned disc width DW and disc length DL, as well as cranial width CW (defined by Notarbartolo Di Sciara [15] as the maximal dorsal width between antorbital processes). We developed a hierarchical multivariate model for several purposes, including to estimate the true value of the measurements of these three dimensions from replicate drone measurements, to examine the correlations between these three dimensions, and to predict the notoriously difficult-to-measure DW from the drone measurements of other dimensions (CW and DL) (Figure 1), while also dealing with imperfect drone measurements associated with errors and uncertainties. The “true value” of a given measurement is defined as “the actual value that would be obtained with perfect measuring instruments and without committing any error of any type in collecting primary data” [35]. Finally, we report upon our initial efforts to use drones to determine the sex and maturity status of surface-feeding *M. alfredi*.

2. Materials and Methods

2.1. Study Area

This study was performed in the Raja Ampat Archipelago, West Papua, Eastern Indonesia (Figure 2). This region covers ~4.5 million ha and is home to large populations of both *M. alfredi* and oceanic manta rays (*M. birostris*) [36,37] that have been fully protected in this region since 2012 [38]. The surveys were conducted in five areas of Raja Ampat: Wayag lagoon, Yefnabi Kecil fringing reef, the Fam islands, Hol Gam bay, and the patch reefs east of Arborek island (Dampier Strait) (Figure 2). These five areas are all well protected from significant wave action and frequently host adult and/or juvenile *M. alfredi* surface feeding or cruising in calm water conditions that are ideal for drone photogrammetry [37,39].

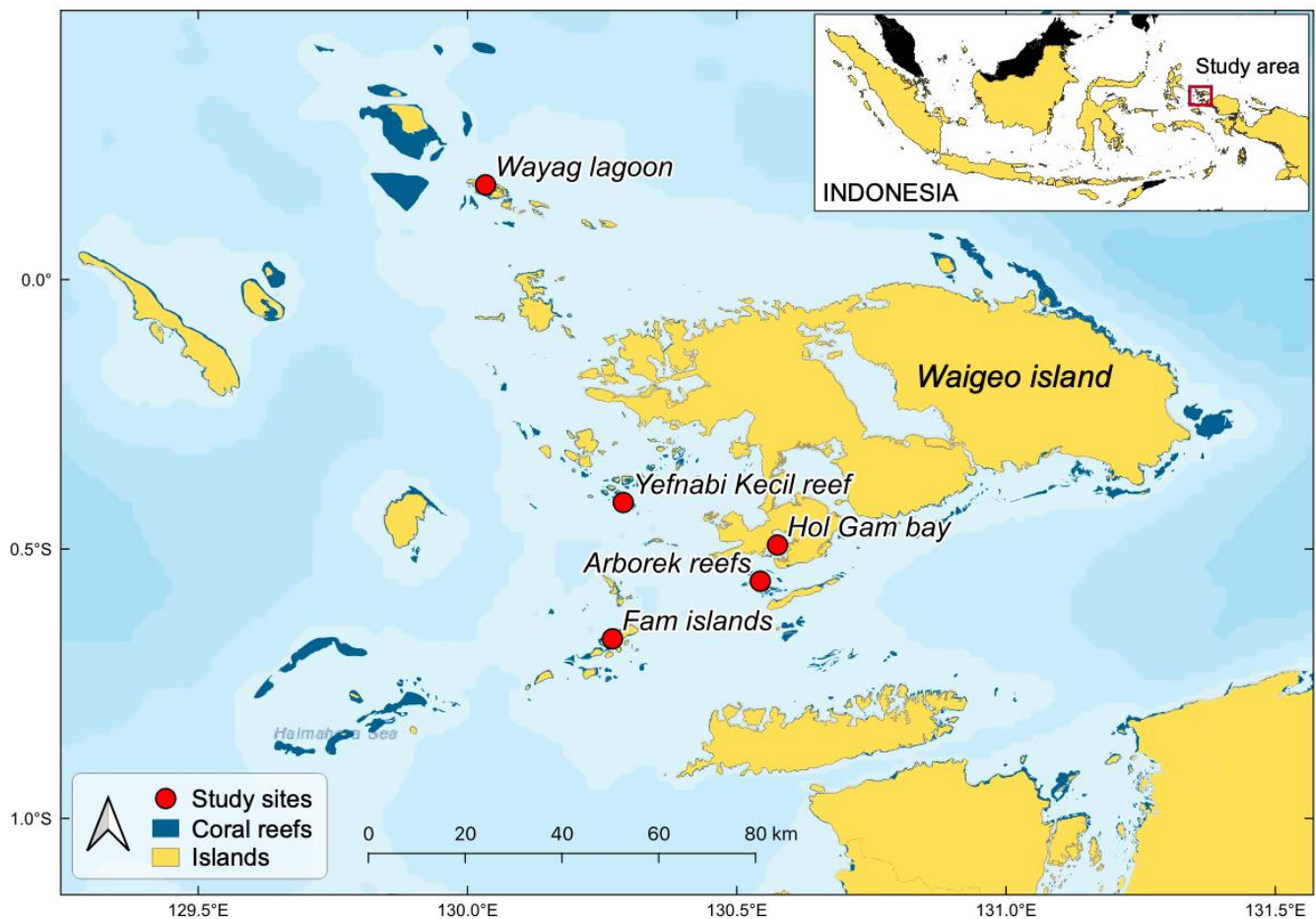


Figure 2. Study sites (red dots) in Northern Raja Ampat archipelago, West Papua, Indonesia.

2.2. Data Collection

Aerial video footage of *M. alfredi* were taken using two units of small, commercially available DJI Mavic 2 Pro drones during boat surveys in January–February 2020 and May–August 2021. Only one drone was used at one time during data collection. The drone was hand-launched from a boat, and then positioned at an altitude of 5–15 m above *M. alfredi* that were feeding or cruising on the surface. The drone camera was tilted to 90° vertically to obtain high-resolution 4K video footage of the *M. alfredi* with a reference scale comprising a 2-m floating PVC pipe placed in the water in the vicinity of the animals. Video clips were generally 15–60 s long, with the camera recording during the periods when the manta ray(s) were at the surface, with the reference pipe included in the field of view (Figure 3).

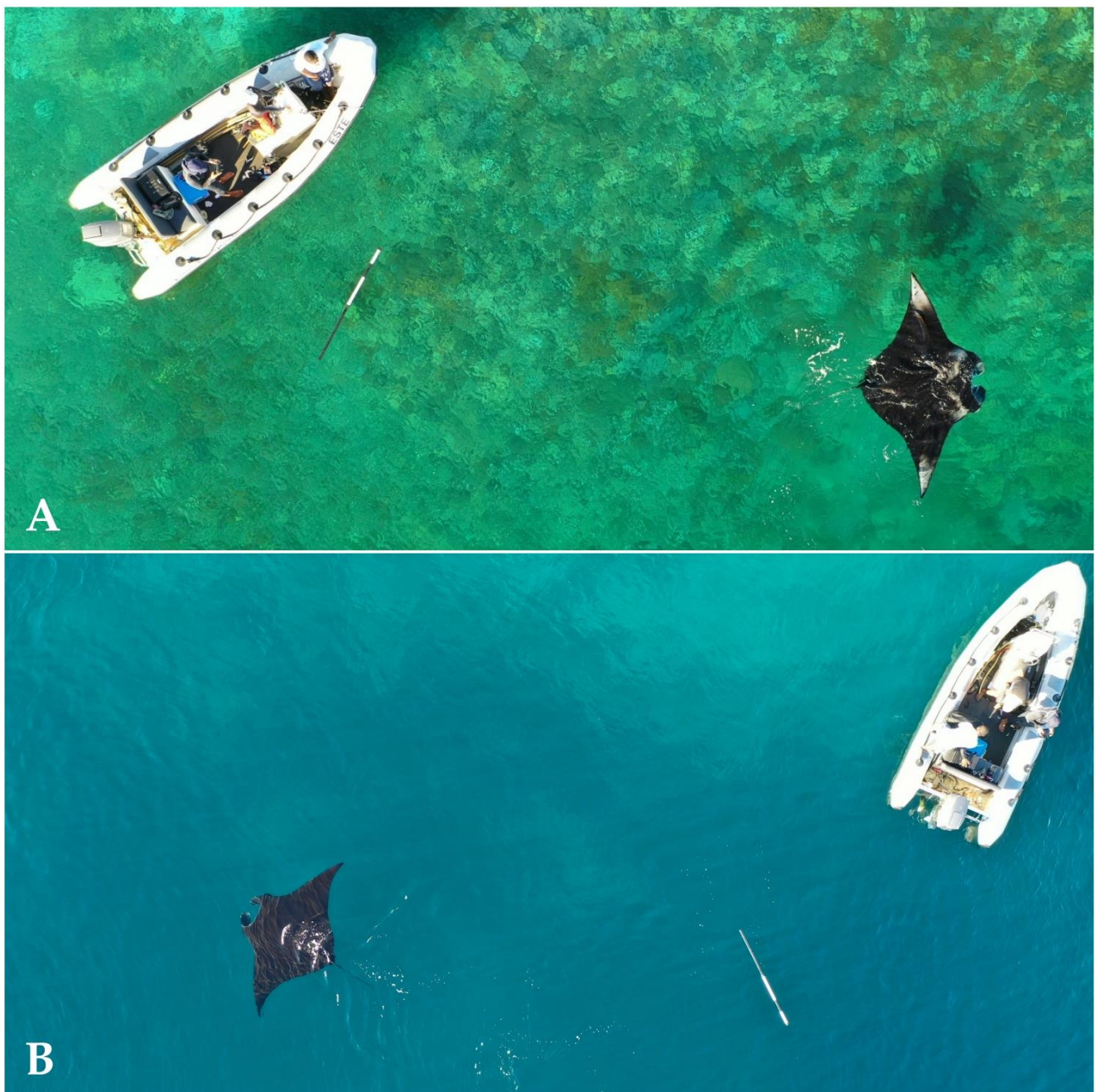


Figure 3. Surface-feeding (A) mature chevron female and (B) melanistic unsexed individual *M. alfredi* and the 2-m floating black-and-white PVC reference pipe as observed from a drone (research boat also visible in frame).

2.3. Image Processing and Measurements

The footage was extracted using Final Cut Pro software to obtain multiple still images of each manta ray at those moments when its pectoral fins were fully extended (to allow the accurate measurement of DW; see Figure 1). We only included manta rays in our analysis, from which we were able to extract and measure at least two separate “wing spread” still images. The measurements were undertaken using the open-source software Tracker (<https://physlets.org/tracker/> (accessed on 1 March 2021)) [40]. The dimensions of each *M. alfredi*, including the DW, DL, and CW, were measured to 1-cm resolution (Figure 1). The three dimensions were measured simultaneously from each image, and this procedure

was then repeated 2–10 times for the same individual, using each of the appropriate frames, showing full pectoral fin extension extracted from the footage.

2.4. Demographic Parameters

In addition to the morphometric dimensions of *M. alfredi*, we opportunistically recorded key demographic parameters of the measured individuals, specifically sex and evidence of maturity. The sex of a manta ray is typically determined in ventral view by divers or snorkelers, with the presence of claspers indicating a male and a cloaca indicating a female [12]. Males are considered mature when their claspers are enlarged and calcified and extend posteriorly beyond the pelvic fins [5], a morphological feature that is readily observed from a dorsal view (Figure 4; [37]). While the cloaca of a female manta ray is not visible in dorsal view, the mating scars on the left-wing, a clear sign of a mature female [12], are clearly visible (Figure 4; [37]). For each animal measured, we recorded whether they were mature using the criteria above. Manta rays with neither visible claspers nor mating scars were recorded as unsexed individuals.

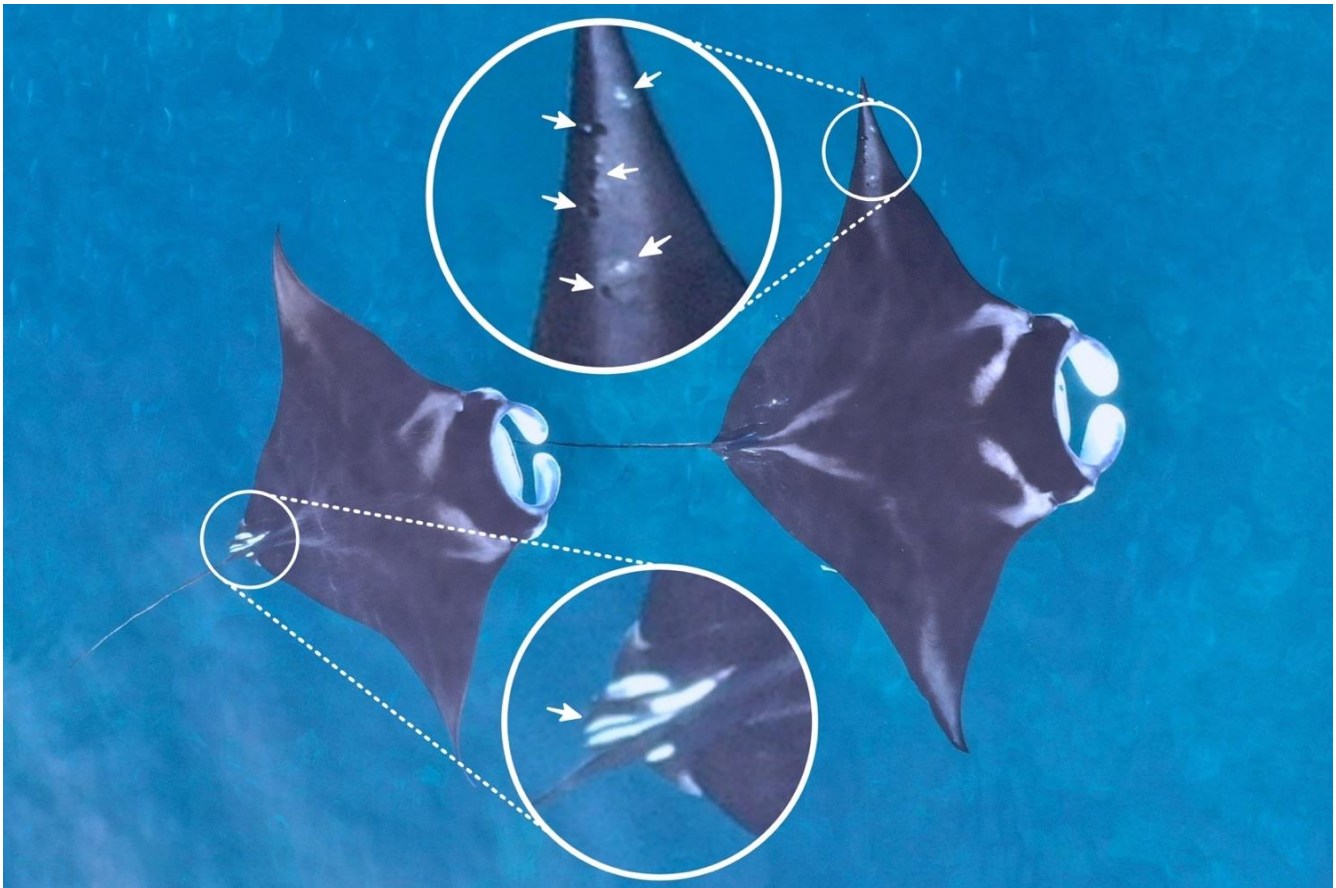


Figure 4. A mature chevron male *M. alfredi* (left) with claspers (white coloration) extended beyond pelvic fins and a mature chevron female (right) with mating scars (black-and-white marks) on her left wing.

2.5. Statistical Analysis

We used a multivariate mixed-effects model (alternatively known as a multivariate hierarchical model) to analyze our data, which we describe in detail in Appendix A. See Bolker et al. [41] and Zuur et al. [42] for overviews of mixed-effects models in ecology. Such models are commonly used when multiple observations are taken from each individual, and when the goal is to estimate the distribution of random effects across individuals, as well as the variance between observations from the same individual.

In our case, we obtained multiple photographs (or multiple still images extracted from footage) of each individual manta ray. Our random effects were the unobserved, true morphometric measurements of the individuals, so we estimated the distribution of the true morphometric measurements across the manta rays in the population. Additionally, observed measurements varied between different photographs of the same individual due to measurement error. Note that here we define measurement error as the unobserved difference between a single measurement from a photograph and the true measurement of the manta ray. Repeated measurements from different photographs of the same manta ray allowed us to estimate the variance of measurement errors without observing the true manta ray measurements. One important assumption required by our model is that the drone measurements are unbiased: although they are not exactly correct due to measurement error, on average they are equal to the true measurement.

One additional distinction between our model and a standard mixed-effects model is that ours is multivariate: we measured three different dimensions from each photograph, so we estimated correlations between the true measurements in addition to the distributions of each individual dimension in the population. All analyses were conducted using R [43], with the code and data included in the Supplementary Data.

We fitted two models to our data. First, we analyzed all manta rays as a single group, estimating parameters for the population as a whole. Second, we fitted a model to analyze data from only the sexually mature individuals. We estimated separate parameters for the distributions of the males' and females' morphometric dimensions, but assumed the measurement error parameters were the same for both groups.

3. Results

3.1. Measurement Summary, Accuracy, and Precision

A total of 86 individual *M. alfredi* were measured using drones from five areas: Arborek reefs ($n = 53$ individuals), Hol Gam bay ($n = 6$), Fam ($n = 11$), Yefnabi Kecil reef ($n = 14$), and Wayag lagoon ($n = 2$). These individuals consisted of 30 sexually mature males, eight sexually mature females, and 48 unsexed individuals. A total of 507 measurements of the three dimensions (DW, DL, and CW) were performed on all the individuals. We fitted our model to examine the population-level parameters for all the manta rays combined and to estimate the true measurements of these three dimensions for all the individuals (summarized in Table S1). Among all the individuals, the smallest animal was an unsexed individual estimated at 206.8 cm DW (95% CI: 204.9–208.6), while the largest was a female estimated at 375.6 cm DW (95% CI: 373.2–378.0).

Additionally, we estimated the population-level parameters for sexually mature individuals separately for each sex. Although we fitted our model to three groups (mature males; mature females; and unsexed individuals, presumably immature individuals), we were primarily interested in comparisons between sexually mature males and females, so we only present these results here for brevity. The model estimated that the mean DW of the sexually mature males (290.1 cm, 95% CI: 286.9–293.4) was smaller than that of the sexually mature females (353.4 cm, 95% CI: 343.7–363.1). The population standard deviations of the three dimensions for the sexually mature males, moreover, were smaller than those for the sexually mature females (Table 1).

The probability density of drone measurement error showed high accuracy for each dimension, with an estimated standard deviation (SD) of 1.13 cm for CW (95% CI: 1.06–1.21), 1.69 cm for DL (95% CI: 1.58–1.80), and 2.16 cm for DW (95% CI: 2.01–2.30) (Table 1, Figure 5). These estimated standard deviations were very small relative to the estimated means of these dimensions for the total population of manta rays (0.75% as large for DW; 1.30% for DL; and 1.52% for CW).

Table 1. Estimates of model parameters, including standard errors (SE), and 95% confidence intervals (CIs) for all individual manta rays combined and for sexually mature males and females separately. The model parameters consisted of population mean (μ) for the dimensions for each demographic group, population standard deviations (σ) for the dimensions for each demographic group, population correlation between two dimensions (ρ) for each demographic group, and standard deviation of measurement error (ψ) for each dimension. DW = disc width, DL = disc length, and CW = cranial width.

Demographic Group	Model Parameters	Estimates	Standard Error (SE)	95% CIs	
				Lower	Upper
All manta rays combined ($n = 86$)	μ_{DW}	286.5	4.87	277.0	296.1
	μ_{DL}	129.8	2.54	124.8	134.7
	μ_{CW}	74.3	1.37	71.6	77.0
	σ_{DW}	45.1	3.44	38.4	51.9
	σ_{DL}	23.5	1.79	20.0	27.0
	σ_{CW}	12.7	0.97	10.8	14.6
	$\rho_{DW,DL}$	0.99	0.003	0.982	0.993
	$\rho_{DW,CW}$	0.99	0.003	0.980	0.991
	$\rho_{DL,CW}$	0.98	0.004	0.977	0.991
	ψ_{DW}	2.16	0.07	2.01	2.30
	ψ_{DL}	1.69	0.06	1.58	1.80
ψ_{CW}	1.13	0.04	1.06	1.21	
Sexually mature males ($n = 30$)	μ_{DW}	290.1	1.7	286.9	293.4
	μ_{DL}	131.1	0.9	129.3	132.8
	μ_{CW}	75.2	0.4	74.4	76.1
	σ_{DW}	9.0	1.2	6.7	11.3
	σ_{DL}	4.8	0.6	3.5	6.0
	σ_{CW}	2.4	0.3	1.8	3.0
Sexually mature females ($n = 8$)	μ_{DW}	353.4	4.9	343.7	363.1
	μ_{DL}	167.3	3.1	161.2	173.3
	μ_{CW}	93.5	1.7	90.1	96.9
	σ_{DW}	13.9	3.5	7.1	20.8
	σ_{DL}	8.7	2.2	4.4	13.0
	σ_{CW}	4.8	1.2	2.4	7.2

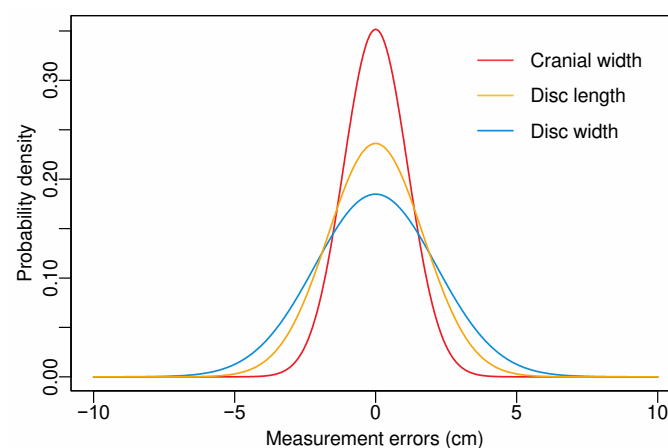


Figure 5. Probability density of drone measurement errors for each dimension (DW, DL, and CW).

3.2. Relationships between Measured Dimensions

Each pairing of DW, DL, and CW for all individual *M. alfredi* measured using drones and estimated using our model in this study was strongly linearly correlated, with estimated coefficients of correlation ranging between 0.98 and 0.99 (Table 1, Figure 6). The correlation between DW and DL was the highest of the dimension pairings, with 0.99 (95%

CI: 0.982–0.993), although the correlation between DW and CW was nearly identical, at 0.99 (95% CI: 0.980–0.991).

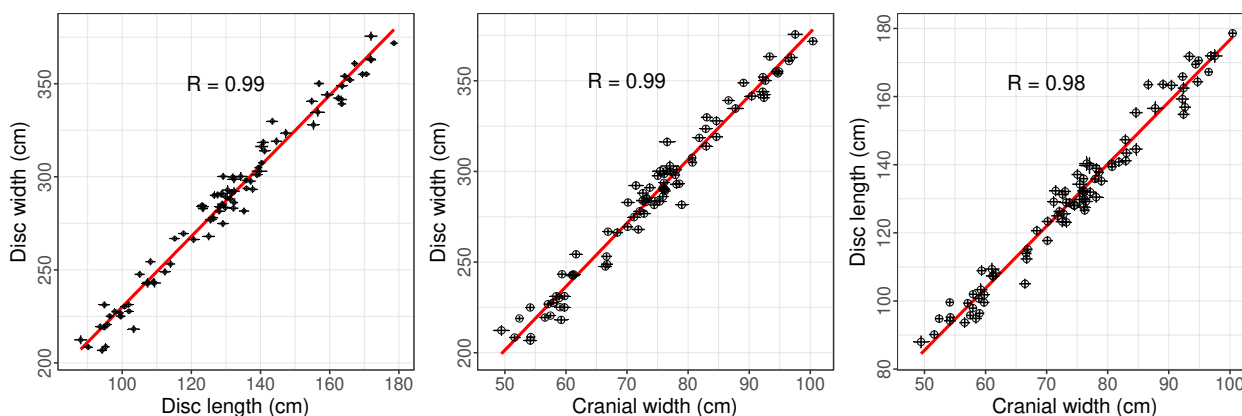


Figure 6. Correlation between each pairing of disc width (DW), disc length (DL), and cranial width (CW) for all individual *M. alfredi* measured using drones and estimated using our model. Black circles represent estimated measurements of each manta ray; horizontal and vertical lines crossing the circles represent the confidence intervals of estimated true measurements of each individual.

We also calculated estimated ratios of the various dimensions for each individual (DW:DL, referred to as “Disc Ratio” or DR by Deakas [5], as well as DW:CW and CW:DL) using their estimated sizes from our model. We fitted a linear model, using these estimated ratios as the response variable and the estimated DW as the explanatory variable. For this secondary analysis, we assumed that our estimated ratios and DW measurements would have negligible errors. We deemed this assumption to have been confirmed, given the very narrow 95% CIs of the estimated true measurements from our hierarchical multivariate model (Table S1).

The linear model showed a clear negative correlation between each ratio and DW (Figure 7). DW explained about 37% of the variation in the DW:DL ratio, but it only explained about 14% of the variation in the DW:CW ratio. Taken together, these negative correlations suggest that *M. alfredi* have a faster rate of growth in the DL dimension than in the DW or CW dimensions, becoming relatively slender as they grow longer. This is commonly described as negative allometric growth [44]. Moreover, our results suggest that the growth rate of CW is faster than that of DW.

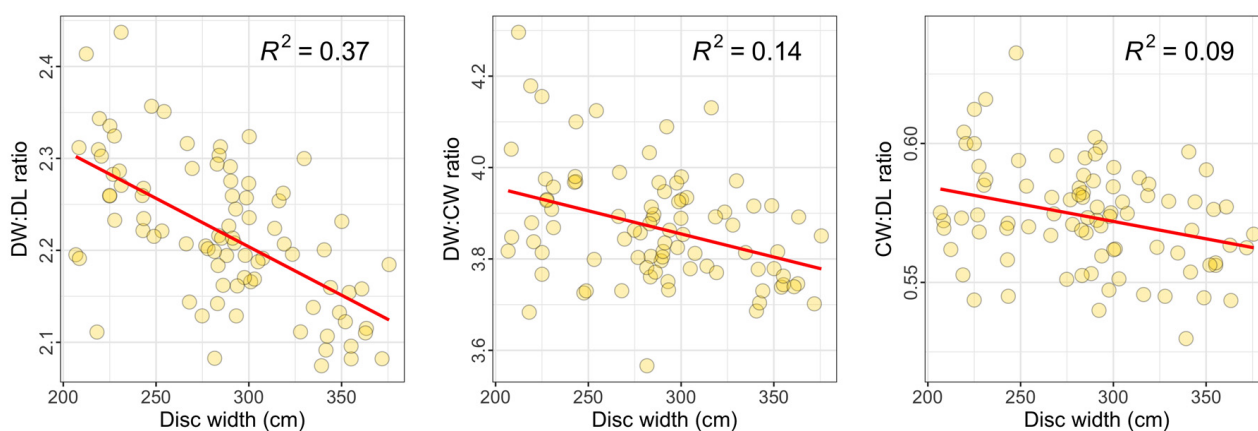


Figure 7. Correlations between DW and DW:DL, DW:CW, and CW:DL ratios of *M. alfredi* measured using drones.

3.3. Using the Model to Predict Unmeasured DW from Other Measured Dimensions

Given the strong linear relationships between the dimensions of the *M. alfredi*, our models allow the prediction of unmeasured dimensions from other measured dimensions. Here, we provide an example of predicting the otherwise difficult-to-measure DW for 13 different individuals using drone-based measurements of either CW alone or DL and CW from these individuals (Figure 8). The 95% confidence intervals of predicted DWs based on the CW measurements alone were wider than those of the drone-based measurements of both CW and DL, indicating that DW is most accurately predicted for a given individual using a model that incorporates measurements of both CW and DL.

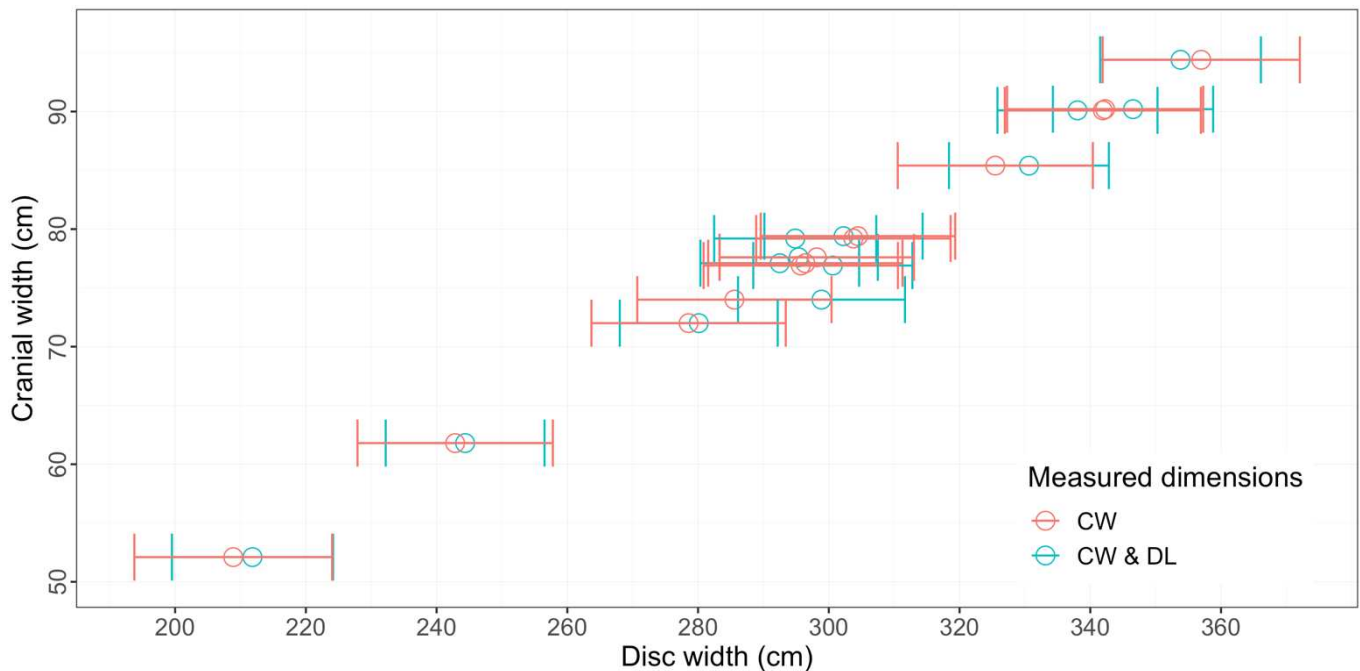


Figure 8. The estimated true measurements of DW predicted using a single drone measurement of CW (red) and drone measurements of both CW and DL (blue) with 95% confidence intervals shown from 13 individuals measured from drones.

3.4. Size at Maturity and Evidence of Sexual Dimorphism

Forty-five percent (39 of 86) of the individual *M. alfredi* measured displayed visible signs of maturity observable from our drones. We estimated that the smallest male with claspers visibly extending posteriorly beyond the pelvic fins was 274.8 cm DW (95% CI: 272.9–276.7), while the smallest female with visible mating scars was 323.5 cm DW (95% CI: 321.6–325.4) (Table S1). By contrast, we estimated that the largest sexually mature male was 316.3 cm DW (95% CI: 313.9–318.7), and that the largest sexually mature female was 371.8 cm DW (95% CI: 370.4–373.2).

The three morphometric dimensions taken for the 30 mature males and eight mature females showed no overlap in any of the measurements, with the smallest mature female recorded having larger dimensions than the largest male (Table S1, Figure 9). Using the most common measurement of body size in manta rays, the mean DW of the sexually mature females (353.4 cm; 95% CI: 343.7–363.1) was significantly ($p < 0.001$) larger than that of the sexually mature males (290.1 cm; 95% CI: 286.8–293.4) estimated in our study (Table 1).

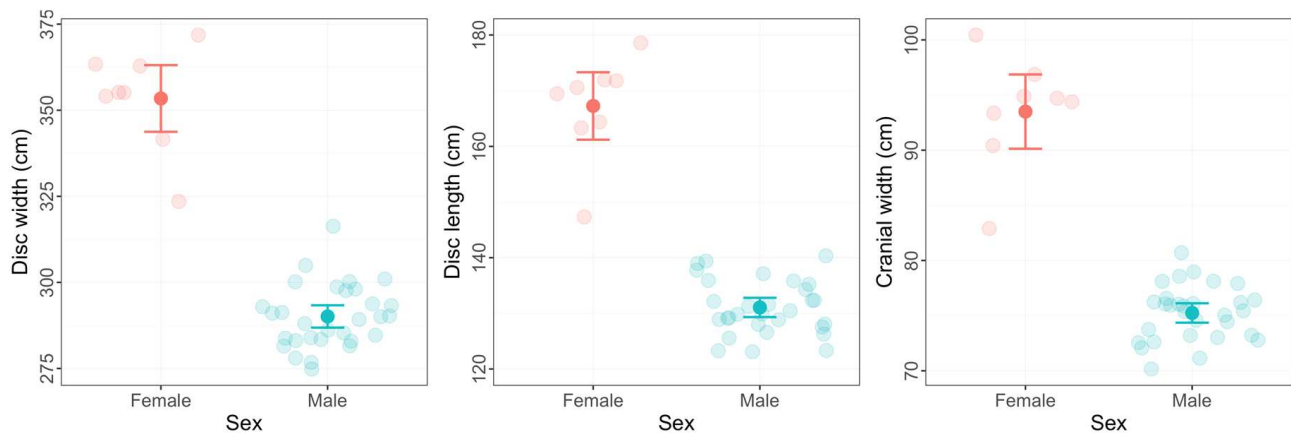


Figure 9. Estimated mean DW (in cm) with 95% confidence intervals of sexually mature female ($n = 8$; solid red circle with CI) and male ($n = 30$; solid blue circle with CI) *M. alfredi* measured using drones and estimated by our model. The transparent circles represent the estimated true measurements of the DW of each individual, color-coded by sex.

4. Discussion

Drones have been increasingly used in elasmobranch research in the last few years to study the abundance, habitat use, fine-scale movements, feeding and social behaviors of various shark and ray species [45,46] including manta rays [37,47]. Here, we show that it is possible to reliably measure the size of manta rays using small, commercially available drones, and present a model for use in other studies. Paired with visual signs of sexual maturity from drone images, we were able to advance our understanding of the population demographics of *M. alfredi* in Raja Ampat. Recently, Oleksyn et al. [48] published the first study using drones to measure the body size of an elasmobranch, the short-tailed stingray, *Bathytoshia brevicaudata*. Our study is the first, to our knowledge, to describe a method for measuring the body size of manta rays using drones. Our methodology differs significantly from that utilized by Oleksyn et al. [48] and other studies using drones to measure whales [31–33,49]. The morphometric measurements in each of those studies were calculated using the known size of the drone’s camera sensor (i.e., width in pixels) and the altitude reported by the drone at the time the image was recorded, with the drone altitude derived from onboard barometric or laser altimeters. However, barometric altitude measurements from drones are known to have poor accuracy due to their sensitivity to rapid changes in air pressure unassociated with the changes in drone altitude, such as wind gusts or other atmospheric conditions [50]. In our study, we used small drones (the same as used by Oleksyn et al. [48]) equipped with low-cost sensors that are reported to have severe issues in drift and delay in their barometric altitude readings [51]. To avoid the measurement error related to this uncertainty, we used a known length object as a scale within the same frame to measure the size of the manta rays. This is similar to the approach of Christiansen et al. [1], who used a research vessel as a scale to measure humpback whales, *Megaptera novaeangliae*, utilizing this scale photograph to convert the relative measurement (in pixels) obtained from different photographs into absolute measurements (in cm). However, instead of using different still images as a scale photograph, we use the same photograph with a floating PVC pipe as a reference scale to measure the manta ray body size. This approach provides more robust measurements, particularly when using low-cost drones with high uncertainty in altitude readings.

Nonetheless, even when using objects of known size as a reference, drone photogrammetry is subject to uncertainties resulting from image processing and variations in body size between individuals in a population [31,49]. While dealing with these sources of uncertainty, our model accurately estimated the measurements of the animals in our study. Similar to our method, Bierlich et al. [34] developed a Bayesian model to predict drone morphometric measurements of whales while considering various uncertainties. Both this

model and ours have the ability to estimate the predictive distribution of a measurement, instead of a single value, providing more robust information about individuals and populations. The ability to predict population-level morphological relationships and to predict unmeasured dimensions of marine animals based on parameter estimates derived from a model is an important advancement in the use of photogrammetry. Importantly, our method is able to estimate an expected value of any dimension using any combination of the other dimensions based on the coefficients calculated by a single fitted model. Our model can accommodate any number of dimensions of interest, and is therefore widely applicable to a variety of studies.

While the most commonly used methods for estimating or measuring the dimensions of manta rays require divers/observers to be in the water [5,12,14], our method offers an alternative, non-invasive approach, requiring no in-water interaction and having minimal or no impact on the animals. The only impact observed using our method was related to the floating PVC pipe. Most of the time, the manta rays showed no reaction towards the pipe floating near them, particularly when it remained outside of the animals' swimming paths while they were feeding. The manta rays displayed some minor, short-term avoidance behavior when the pipe floated directly into their swimming path, in which case they would either submerge beneath the pipe and then resurface as the pipe passed over them, or swim laterally around the pipe and then recommence their feeding behavior.

4.1. Accuracy and Measurement Methods

The drone measurements of the surface-feeding or cruising *M. alfredi* were highly accurate and precise. The estimated standard deviation of measurement error using our approach was less than 2.2 cm for each of the dimensions, which is extremely small relative to the true measurements. The precision of our measurements of the manta rays' dimensions was higher than that derived from paired laser photogrammetry in Hawaii, which is promising as researchers endeavor to improve measurement accuracy [5]. Importantly, the precision of our drone measurement was comparable to work on southern right whales, *Eubalaena australis*, using a larger DJI Inspire 1 Pro equipped with LIDAR to measure altitude [33]. It is encouraging that the data we collected with the smaller, more affordable Mavic Pro drone provided reliable results.

Of the three dimensions we measured, CW was the most accurate, while the measurements of DW were the least accurate. The larger variability in the DW measurements was likely due to the difficulty of capturing images of manta rays at exactly the moment of maximum extension of the pectoral fins when swimming—a difficulty also discussed by Deakos [5] when using paired laser photogrammetry in Hawaii. Burnett et al. [31] suggest that errors in measurement with aerial photogrammetry of marine animals in general may come from a combination of various factors, including inaccurate readings of relative altitude by the drone, animal body flex, and animal bodies that are partially submerged in water. In our study, we did not utilize altitude readings, and we only took video measurements when the manta rays were clearly surface-feeding or cruising in calm water conditions. Body flex, however, is another means of describing the difficulty of capturing the manta ray with maximum wing extension, and is one of the main reasons why Francis [23] suggested that DW has more measurement errors than other dimensions and should be replaced by DL as the primary measurement used for describing body size in mobulid rays. While our drone measurements indicated that DW had the smallest standard deviation relative to the mean body size, CW and DL are easier to measure in practice, with CW being the most accurate. Therefore, we suggest that CW should be considered as a primary metric in describing manta ray body size when using a drone, considering that these measurements can be established accurately using our model. We acknowledge that standard scientific convention most commonly uses DW to describe manta ray body size, in which case our model offers the ability to accurately predict DW from measurements of either CW or DL (or preferably, both). Importantly, this approach of

using CW or DL to calculate DW can be applied not only to drone measurements, but also to the aforementioned in-water estimation/measurement methodologies for manta rays.

4.2. Allometric Growth, Size at Maturity and Sexual Dimorphism

One of the more unexpected findings of our study was the negative allometric growth. Deakos [5] previously reported that *M. alfredi* show isometric growth, which is unusual in fishes, but our data show that *M. alfredi* in Raja Ampat become relatively slender (as measured by either DW or CW) as they grow longer, reflecting clear negative allometric growth [44]. Of the three morphometric dimensions we considered, each had different growth rates. DL had the fastest growth rate, followed by CW, with DW experiencing the slowest rate of growth of the three dimensions. Nonetheless, despite the differences in growth rates, each pairing of dimensions showed a very strong linear correlation across the range of body sizes we measured, thereby conveniently allowing the calculation of one unmeasured dimension from the other measured dimensions.

While our sample size of 86 individual *M. alfredi* is not large enough to confidently describe the demographic parameters of the large Raja Ampat population [37], we were nonetheless able to record some valuable observations that are worth comparing to the *M. alfredi* from across their Indo-Pacific distribution. The largest animal estimated in our study was a 375.6 cm DW female, which is similar to other studies, such as those in Hawaii, the Maldives, and the Seychelles, using different techniques [5,12,14].

The adult or sexually mature male and female *M. alfredi* were determined by the morphological features [12,16] observed in the drone imagery when surface-feeding. We estimated that the smallest sexually mature male was 274.8 cm DW (95% CI: 272.9–276.7), while the smallest sexually mature female was 323.5 cm DW (95% CI: 321.6–325.4). These findings are consistent with studies from Hawaii [5] and the Maldives [12]. In the Maldives, males were estimated to reach maturity at approximately 270–280 cm DW and females at approximately 320–330 cm DW [12]. In Japan, however, they are considerably larger, with females estimated to mature at 380–400 cm DW and males at 280–300 cm DW [52].

We found strong evidence of sexual dimorphism in body size of *M. alfredi*, with adult females larger than adult males in all three morphometric dimensions measured. This finding is similar to those in several other regions [5,12,16,53]. This is likely related to female *M. alfredi* requiring a larger body to gestate their large, precocial pups [54,55].

4.3. Limitations of the Methodology

Despite its utility, we nonetheless recognize some important limitations of our method. First, it is only useful for measuring manta rays that are surface-feeding or cruising at the surface in calm water conditions. While this limits its utility, our experience of using drones to observe *M. alfredi* throughout Indonesia, Papua New Guinea, and New Caledonia and *M. birostris* in New Zealand suggests that these conditions are met at least part of the time in each of these areas, such that the methodology should be broadly applicable.

A more important limitation of the methodology is that the measurements collected cannot necessarily be attributed to individuals that are tracked over time in the same manner as the other in-water methods of measurement. *M. alfredi* have uniquely identifiable ventral spot patterns that enable the collection of photographic images, which can be collated in a database and allow the tracking of individuals over time [12,37,56]. In the studies using visual estimation, paired laser photogrammetry, or estimation with paired stereo video cameras to measure the size of *M. alfredi*, a key advantage is that these methods include the linking of the measurements obtained with a photo-ID image of the manta ray. This in turn allows researchers to obtain repeated measurements of the same individuals and, thereby, calculate growth rates. We note, however, that it is often possible to link drone measurements to an individual if the manta ray being measured performs somersault feeding near the surface, which allows excellent identification images to be taken [37] at the same time as measurements are collected. Somersault feeding is particularly common in our experience with juvenile *M. alfredi* in nursery areas in Raja Ampat [37] and with

M. birostris feeding offshore of New Zealand [57], and may very well be common in other localities, depending on the oceanographic conditions and planktonic prey behaviors.

Finally, while our drone-based methodology did allow the collection of opportunistic observations on the sex and maturity status of the individuals being measured, we were not able to reliably determine this for all the manta rays we encountered. It is impossible to determine the sex of a juvenile manta ray from a drone unless the individual happens to be somersault feeding [37]. For sexually mature males, we are able to very reliably identify the claspers extending beyond the pelvic fins using drone photogrammetry, which will allow us to produce highly accurate estimates of size at maturity for males in a given population.

Maturity in females, however, has proven much more difficult to reliably measure with drones. Using Steven's [12] estimate of size at maturity for Maldivian female *M. alfredi* with 320–330 cm DW (from the most comprehensive study yet published on *M. alfredi* demographic characteristics), we observed 17 individuals that were over 330 cm DW and did not show extended claspers in the dorsal view; thus, they could reasonably be assumed to be adult females. However, we only observed mating scars from a dorsal view on 41% of these individuals. Importantly, seven of the ten large females on which we did not observe mating scars were melanistic individuals; the lack of white shading on the dorsal wing tips (compare to Figure 4 for a normal “chevron” colored female) of these melanistic females made it much more difficult to observe any evidence of mating scars (Setyawan, pers. obs.). The remaining three large chevron-colored females with no visible dorsal mating scars either had not previously mated, only showed mating scars ventrally, or had healed their mating scars to the point that they could not be recognized. Whatever the reason, it is clear that drone photogrammetry is limited in its ability to identify females and sexual maturity in females, except when these females perform somersault feeding and allow a ventral view of their cloaca and pectoral fins.

5. Conclusions

We demonstrated conclusively the value of using small, commercially available drones to accurately measure the body size of surface-feeding or cruising *M. alfredi* with minimal or no impact on the animals. The three morphometric dimensions of *M. alfredi* measured using drones in this study (DW, DL, and CW) were strongly linearly correlated, allowing us to develop models that can predict an unmeasured or less accurately measured dimension (such as DW) using drone measurements of CW, DL, or, preferably, both. We also showed that drones can be used to determine sexually mature individuals, a key demographic parameter useful for conservation management [12]. Finally, we found evidence of sexual dimorphism in body size (with females significantly larger than males) and negative allometric growth (with growth rates for $DL > CW > DW$).

Although our method can only be used on surface-feeding or cruising manta rays in relatively calm waters, if the individual is somersault feeding at the time of measurement, we can also individually identify the animal and more accurately assign sex to females that are difficult to identify from the dorsal view. Importantly, our drone-based methodology is beneficial for providing an accurate “snapshot” of the size distribution of *M. alfredi* aggregations, and for reliably determining size for mature male individuals. Moreover, our robust models for calculating DW from either CW or DL measures (or, more accurately, both) should be equally useful for in-water measurement techniques, including paired laser photogrammetry and estimation by paired stereo video cameras.

In the future, this novel method can be used to identify *M. alfredi*'s critical habitats, such as nursery areas, by determining the size distribution of neonates and juveniles occupying the nursery. In combination with photographic identification, this method can be used to accurately estimate the growth rate of manta rays. Importantly, given the simplicity of the data collection and the functionality of the data analysis, this method is easily replicable to measure the body size of manta ray populations in other countries and possibly that of other marine megafauna species that spend time at the surface.

Supplementary Materials: The following supporting information can be downloaded at: <https://www.mdpi.com/article/10.3390/drones6030063/s1>. Table S1: Estimated true measurements of dimensions (DW, DL, and CW), including the lower and upper 95% confidence intervals (CIs), of each individual *M. alfredi* measured using drones.

Author Contributions: Conceptualization, E.S., R.C. and M.V.E.; data curation, E.S.; formal analysis, E.S. and B.C.S.; funding acquisition, E.S. and M.V.E.; investigation, E.S. and M.I.; methodology, B.C.S.; software, B.C.S.; supervision, B.C.S., R.C. and M.V.E.; visualization, E.S.; writing—original draft, E.S., B.C.S., R.C. and M.V.E.; writing—review and editing, E.S., B.C.S., M.I., R.C. and M.V.E. All authors have read and agreed to the published version of the manuscript.

Funding: This research was funded by WWF's Russell E. Train Education for Nature Program (EFN), grant number RH81. The fieldwork was also financially and logistically supported by MAC3 Impact Philanthropies. The APC was funded by the Wolcott Henry Foundation.

Institutional Review Board Statement: Ethical approval to conduct this study was granted by the University of Auckland Animal Ethics Committee (AEC) to R.C., under protocol 002228, on 31 January 2020. The Raja Ampat Archipelago Marine Protected Areas (MPAs) Management Authority (UPTD-BLUD KKPJ Raja Ampat) also granted permission to conduct the research.

Data Availability Statement: The data presented in this study are openly available and provided in the Supplementary Data to this article.

Acknowledgments: We thank the Government of Indonesia (including the Ministry of Marine Affairs and Fisheries and the Ministry of Environment and Forestry), the West Papua Conservation Agency (BBKSDA Papua II), the Raja Ampat MPA Management Authority (UPTD-BLUD KKPJ Raja Ampat and BKKPN Kupang Satker Raja Ampat) and the people of Raja Ampat for hosting this work. We thank the following donors for their generous support for this project: MAC3 Impact Philanthropies, Daniel Roozen, the Stellar Blue Fund, and the Wolcott Henry Foundation. We extend a warm thanks to Ronald Mambrasar, Orgenes Ambafen, Yaswal's captain Urias Tuhumena, Demas Fiay, Immanuel Mofu, Iqbal Herwata, Abdi W. Hasan, and Maulana Nugraha for their support and tireless effort in assisting data collection in the field. The first author was awarded a New Zealand Scholarship (NZAS) to undertake a doctoral program at the University of Auckland and thanks the Global Fellowship in Marine Science for the opportunity to undertake the summer school on drones for conservation at Nicholas School of the Environment, Duke University Marine Lab. Lastly, we also note that this research was made possible thanks to funding for the first author from WWF's Russell E. Train Education for Nature Program (EFN).

Conflicts of Interest: The authors declare no conflict of interest.

Appendix A

In general, we consider a situation in which we have drone measurements of m morphometric dimensions belonging to G different groups, where n_g unique individuals have been measured from the g th group. In our specific case here, we have $m = 3$ morphometric dimensions. For our first model, we analyzed all the manta rays as a single group, so $G = 1$. For our second model, we grouped the individuals into $n_1 = 30$ sexually mature males, $n_2 = 8$ sexually mature females, and $n_3 = 48$ unsexed individuals, so for this analysis $G = 3$.

Let p_{gi} be the number of drone images captured of the i th animal in the g th group. For this animal, we observe an $p_{gi} \times m$ matrix Y_{gi} . The element in the j th row and k th column, y_{gijk} , is a measurement of the k th morphometric dimension in the j th image, and is subject to measurement error. Let $u_{gi} = (u_{gi1}, \dots, u_{gim})$ be a vector containing the unobserved true morphometric dimensions of the i th individual in the g th group, where u_{gik} is the unobserved true measurement of the k th dimension.

Appendix A.1. True Measurements

We assume $u_{gi} \sim \text{MVN}_m(\mu_g, \Sigma_g)$; that is, individuals in the g th group have true morphometric dimensions that come from a multivariate normal distribution, where $\mu_g = (\mu_{g1}, \dots, \mu_{g2})$ is a vector of the underlying mean measurements for the m dimensions in the group's population, and Σ_g is an $m \times m$ variance–covariance matrix of the

measurements. In this matrix, the k th diagonal element, $\Sigma_{gkk} = \sigma_{gk}^2$, is the variance of the k th dimension across individuals in the g th group's population, while the off-diagonal element in the k th row and k' th column ($k \neq k'$) is $\Sigma_{gkk'} = \rho_{kk'}\sigma_{gk}\sigma_{gk'}$, the covariance between the k th and k' th dimension. Here, $\rho_{kk'}$ is the correlation between these morphometric dimensions.

Appendix A.2. Measurement Error

We do not observe true measurements, \mathbf{u}_{gi} , which precludes the direct estimation of the mean vector, $\boldsymbol{\mu}_g$, and variance–covariance matrix $\boldsymbol{\Sigma}_g$ for each group. Instead, we observe the matrix \mathbf{Y}_{gi} for each individual, comprising p_{gi} noisy measurements of \mathbf{u}_{gi} that are subject to error. We assume the measurement error distribution is itself multivariate-normal, and so $\mathbf{Y}_{gij} \mid \mathbf{u}_{gi} \sim \text{MVN}_m(\mathbf{u}_{gi}, \boldsymbol{\Xi})$. This assumption implies that drone measurements are unbiased: the underlying mean drone measurement of a particular morphometric dimension is equal to the true measurement. The matrix $\boldsymbol{\Xi}$ is a variance–covariance matrix for the measurement error, where the k th diagonal element, $\Xi_{kk} = \psi_k^2$, is the measurement error variance of the k th dimension, while the off-diagonal element in the k th row and k' th column ($k \neq k'$) is $\Xi_{kk'} = \phi_{kk'}\psi_k\psi_{k'}$, the covariance between measurement errors for the k th and k' th dimensions. Here, $\phi_{kk'}$ is the correlation between the measurement errors for these morphometric dimensions. Note that we assume that measurement errors were the same across all the groups.

Appendix A.3. Model Parameters

The parameters of our model are therefore, the following:

- $\boldsymbol{\mu} = (\boldsymbol{\mu}_1, \dots, \boldsymbol{\mu}_G)$, where $\boldsymbol{\mu}_g$ contains the underlying population means of the morphometric dimensions for the g th group;
- $\boldsymbol{\sigma} = (\boldsymbol{\sigma}_1, \dots, \boldsymbol{\sigma}_G)$, where $\boldsymbol{\sigma}_g$ contains the underlying population standard deviations of the morphometric dimensions for the g th group;
- $\boldsymbol{\rho} = (\boldsymbol{\rho}_1, \dots, \boldsymbol{\rho}_G)$, where $\boldsymbol{\rho}_g$ contains underlying population correlations between all pairs of morphometric dimensions;
- $\boldsymbol{\psi}$ containing underlying standard deviations of the measurement errors for each of the m dimensions; and
- $\boldsymbol{\phi}$ containing underlying correlations between measurement errors of all morphometric dimensions.

The variance–covariance $\boldsymbol{\Sigma}_g$ can be constructed from parameters $\boldsymbol{\sigma}_g$ and $\boldsymbol{\rho}_g$. Likewise, $\boldsymbol{\Xi}$ can be constructed from $\boldsymbol{\psi}$ and $\boldsymbol{\phi}$. Fitting this model therefore accommodates measurement error, because parameter vectors $\boldsymbol{\psi}$ and $\boldsymbol{\phi}$ characterize the distribution of the measurement errors. Our model also allows the inference of the distribution of true, unobserved morphometric measurements, which is characterized by parameter vectors $\boldsymbol{\mu}$, $\boldsymbol{\sigma}$, and $\boldsymbol{\rho}$.

Appendix A.4. Relationships between Dimensions

Fitting a multivariate normal distribution implies that each of the component variables are linearly related to the others. To determine the linear relationships between the true morphometric dimensions in the g th group, we can translate $\boldsymbol{\mu}_g$ and $\boldsymbol{\Sigma}_g$ into coefficients of a linear equation that returns the expected value of one morphometric dimension conditional on the observed values of any combination of the other dimensions. These coefficients can be interpreted in the same way as those from a standard linear regression model, and allow predictions of unmeasured dimensions based on those that have been measured.

Let us imagine that we wish to determine the coefficients of the linear equation to calculate the expected value of dimension p , conditional on observed values of s other dimensions, q_1, \dots, q_s . For example, if we wish to calculate the expected value of the first dimension conditional on observed values of the third and fifth, we have $p = 1$, $s = 2$, $q_1 = 3$, and $q_2 = 5$. Using standard results conditional multivariate distributions, the vector

of coefficients for dimensions q_1, \dots, q_s is given by $\beta = \Sigma_{gA} \Sigma_{gB}^{-1}$, and the intercept is given by $\alpha = \mu_{gp} - \sum_{i=1}^s \beta_i \mu_{gi}$, where Σ_{gA} is the p th row of Σ_g , excluding the p th element, and Σ_{gB} is an $s \times s$ submatrix of Σ_g , containing its q_1 th, \dots , q_s th rows and columns. Therefore, the parameters of our model can be used to determine coefficients for linear combinations to describe the relationships between any subset of the morphometric dimensions.

Appendix A.5. Parameter Estimation

We fit our hierarchical multivariate normal model by maximum likelihood. The likelihood of our model is:

$$L(\theta) = \prod_{g=1}^G \prod_{i=1}^{n_g} \int_{\mathcal{R}^m} f_u(\mathbf{u}_{gi}; \boldsymbol{\mu}_g, \boldsymbol{\sigma}_g, \boldsymbol{\rho}_g) \prod_{j=1}^{p_{gi}} f_{y|u}(\mathbf{y}_{gij} | \mathbf{u}_{gi}; \boldsymbol{\psi}, \boldsymbol{\phi}) d\mathbf{u}_{gi} \quad (\text{A1})$$

where $f_u(\mathbf{u}; \boldsymbol{\mu}, \boldsymbol{\sigma}, \boldsymbol{\rho})$ is the multivariate normal probability density function (PDF) with the mean vector $\boldsymbol{\mu}$ and variance–covariance matrix constructed from marginal standard deviations $\boldsymbol{\sigma}$ and correlations $\boldsymbol{\rho}$. Likewise, $f_{y|u}(\mathbf{y} | \mathbf{u}; \boldsymbol{\psi}, \boldsymbol{\phi})$ is the multivariate-normal PDF with mean vector \mathbf{u} and constructed from marginal standard deviations $\boldsymbol{\phi}$ and correlations $\boldsymbol{\psi}$.

This integrand in Equation (A1) is a Gaussian function, so it is available in closed form. Nevertheless, we wrote code to calculate our model’s likelihood using TMB software [58], which uses the Laplace approximation to evaluate the integral. We used the R function `nlminb()` to numerically maximize the likelihood.

We wrote additional R functions to predict the true measurements of the morphometric dimensions, given either drone measurements of new individuals (i.e., not in our original data set and subject to the same measurement error), true measurements (i.e., not subject to any measurement error), or a combination of both.

References

- Christiansen, F.; Dujon, A.M.; Sprogis, K.R.; Arnould, J.P.; Bejder, L. Noninvasive unmanned aerial vehicle provides estimates of the energetic cost of reproduction in humpback whales. *Ecosphere* **2016**, *7*, e01468. [CrossRef]
- Gray, P.C.; Bierlich, K.C.; Mantell, S.A.; Friedlaender, A.S.; Goldbogen, J.A.; Johnston, D.W. Drones and convolutional neural networks facilitate automated and accurate cetacean species identification and photogrammetry. *Methods Ecol. Evol.* **2019**, *10*, 1490–1500. [CrossRef]
- Perryman, W.L.; Lynn, M.S. Identification of geographic forms common dolphin (*Delphinus delphis*) from aerial photogrammetry. *Mar. Mamm. Sci.* **1993**, *9*, 119–137. [CrossRef]
- Rogers, T.D.; Cambiè, G.; Kaiser, M.J. Determination of size, sex and maturity stage of free swimming catsharks using laser photogrammetry. *Mar. Biol.* **2017**, *164*, 213. [CrossRef] [PubMed]
- Deakos, M.H. Paired-laser photogrammetry as a simple and accurate system for measuring the body size of free-ranging manta rays *Manta alfredi*. *Aquat. Biol.* **2010**, *10*, 1–10. [CrossRef]
- Gaudio, V.; Sanz-Ablanedo, E.; Lomillos, J.M.; Alonso, M.E.; Javares-Morillo, L.; Rodríguez, P. “Photozoomer”: A new photogrammetric system for obtaining morphometric measurements of elusive animals. *Livest. Sci.* **2014**, *165*, 147–156. [CrossRef]
- Schenk, T. *Introduction to Photogrammetry*; The Ohio State University: Columbus, OH, USA, 2005; Volume 106, p. 95.
- Bräger, S.; Chong, A.; Dawson, S.; Slooten, E.; Würsig, B. A combined stereo-photogrammetry and underwater-video system to study group composition of dolphins. *Helgol. Mar. Res.* **1999**, *53*, 122–128. [CrossRef]
- Jeffreys, G.; Rowat, D.; Marshall, H.; Brooks, K. The development of robust morphometric indices from accurate and precise measurements of free-swimming whale sharks using laser photogrammetry. *Mar. Biol. Assoc. UK* **2013**, *93*, 309–320. [CrossRef]
- Menesatti, P.; Costa, C.; Antonucci, F.; Steri, R.; Pallottino, F.; Catillo, G. A low-cost stereovision system to estimate size and weight of live sheep. *Comput. Electron. Agric.* **2014**, *103*, 33–38. [CrossRef]
- Marshall, A.; Barreto, R.; Carlson, J.; Fernando, D.; Fordham, S.; Francis, M.P.; Herman, K.; Jabado, R.W.; Liu, K.M.; Pacoureaux, N.; et al. *Mobula alfredi*. In *The IUCN Red List of Threatened Species 2019: e.T195459A68632178*; 2019; Available online: <https://dx.doi.org/10.2305/IUCN.UK.2019-3.RLTS.T195459A68632178.en> (accessed on 9 April 2021).
- Stevens, G.M.W. Conservation and Population Ecology of Manta Rays in the Maldives. Ph.D. Dissertation, University of York, York, UK, 2016.
- Rambahinarison, J.M.; Lamoste, M.J.; Rohner, C.A.; Murray, R.; Snow, S.; Labaja, J.; Araujo, G.; Ponzio, A. Life history, growth, and reproductive biology of four mobulid species in the Bohol Sea, Philippines. *Front. Mar. Sci.* **2018**, *5*, 269. [CrossRef]
- Peel, L.R.; Stevens, G.M.W.; Daly, R.; Daly, C.A.K.; Lea, J.S.E.; Clarke, C.R.; Collin, S.P.; Meekan, M.G. Movement and residency patterns of reef manta rays *Mobula alfredi* in the Amirante Islands, Seychelles. *Mar. Ecol. Prog. Ser.* **2019**, *621*, 169–184. [CrossRef]

15. Notarbartolo Di Sciarra, G. A revisionary study of the genus *Mobula* Rafinesque, 1810 (Chondrichthyes: Mobulidae) with the description of a new species. *Zool. J. Linn. Soc.* **1987**, *91*, 1–91. [[CrossRef](#)]
16. Marshall, A.D.; Bennett, M.B. Reproductive ecology of the reef manta ray *Manta alfredi* in southern Mozambique. *J. Fish Biol.* **2010**, *77*, 169–190. [[CrossRef](#)]
17. Sequeira, A.M.; Thums, M.; Brooks, K.; Meekan, M.G. Error and bias in size estimates of whale sharks: Implications for understanding demography. *R. Soc. Open Sci.* **2016**, *3*, 150668. [[CrossRef](#)] [[PubMed](#)]
18. Couturier, L.I.E.; Dudgeon, C.L.; Pollock, K.H.; Jaine, F.R.A.; Bennett, M.B.; Townsend, K.A.; Weeks, S.J.; Richardson, A.J. Population dynamics of the reef manta ray *Manta alfredi* in eastern Australia. *Coral Reefs* **2014**, *33*, 329–342. [[CrossRef](#)]
19. Letessier, T.B.; Juhel, J.-B.; Vigliola, L.; Meeuwig, J.J. Low-cost small action cameras in stereo generates accurate underwater measurements of fish. *J. Exp. Mar. Biol. Ecol.* **2015**, *466*, 120–126. [[CrossRef](#)]
20. Harvey, E.; Fletcher, D.; Shortis, M. Estimation of reef fish length by divers and by stereo-video: A first comparison of the accuracy and precision in the field on living fish under operational conditions. *Fish. Res.* **2002**, *57*, 255–265. [[CrossRef](#)]
21. Delacy, C.R.; Olsen, A.; Howey, L.A.; Chapman, D.D.; Brooks, E.J.; Bond, M.E. Affordable and accurate stereo-video system for measuring dimensions underwater: A case study using oceanic whitetip sharks *Carcharhinus longimanus*. *Mar. Ecol. Prog. Ser.* **2017**, *574*, 75–84. [[CrossRef](#)]
22. Murray, A.; Garrud, E.; Ender, I.; Lee-Brooks, K.; Atkins, R.; Lynam, R.; Arnold, K.; Roberts, C.; Hawkins, J.; Stevens, G. Protecting the million-dollar mantas; creating an evidence-based code of conduct for manta ray tourism interactions. *J. Ecotourism* **2020**, *19*, 132–147. [[CrossRef](#)]
23. Francis, M.P. Morphometric minefields—Towards a measurement standard for chondrichthyan fishes. *Environ. Biol. Fishes* **2006**, *77*, 407–421. [[CrossRef](#)]
24. Marshall, A.D.; Pierce, S.J.; Bennett, M.B. Morphological measurements of manta rays (*Manta birostris*) with a description of a foetus from the east coast of Southern Africa. *Zootaxa* **2008**, *1717*, 24–30. [[CrossRef](#)]
25. Last, P.; Naylor, G.; Séret, B.; White, W.; de Carvalho, M.; Stehmann, M. *Rays of the World*; CSIRO Publishing: Melbourne, Australia, 2016.
26. Johnston, D.W. Unoccupied aircraft systems in marine science and conservation. *Ann. Rev. Mar. Sci.* **2019**, *11*, 439–463. [[CrossRef](#)]
27. Landeo-Yauri, S.S.; Ramos, E.A.; Castelblanco-Martínez, D.N.; Niño-Torres, C.A.; Searle, L. Using small drones to photo-identify Antillean manatees: A novel method for monitoring an endangered marine mammal in the Caribbean Sea. *Endanger. Species Res.* **2020**, *41*, 79–90. [[CrossRef](#)]
28. Lyons, M.B.; Brandis, K.J.; Murray, N.J.; Wilshire, J.H.; McCann, J.A.; Kingsford, R.T.; Callaghan, C.T. Monitoring large and complex wildlife aggregations with drones. *Methods Ecol. Evol.* **2019**, *10*, 1024–1035. [[CrossRef](#)]
29. Schofield, G.; Esteban, N.; Katselidis, K.A.; Hays, G.C. Drones for research on sea turtles and other marine vertebrates—A review. *Biol. Conserv.* **2019**, *238*, 108214. [[CrossRef](#)]
30. Torres, L.G.; Nieuwkerk, S.L.; Lemos, L.; Chandler, T.E. Drone up! Quantifying whale behavior from a new perspective improves observational capacity. *Front. Mar. Sci.* **2018**, *5*, 319. [[CrossRef](#)]
31. Burnett, J.D.; Lemos, L.; Barlow, D.; Wing, M.G.; Chandler, T.; Torres, L.G. Estimating morphometric attributes of baleen whales with photogrammetry from small UASs: A case study with blue and gray whales. *Mar. Mamm. Sci.* **2019**, *35*, 108–139. [[CrossRef](#)]
32. Christiansen, F.; Vivier, F.; Charlton, C.; Ward, R.; Amerson, A.; Burnell, S.; Bejder, L. Maternal body size and condition determine calf growth rates in southern right whales. *Mar. Ecol. Prog. Ser.* **2018**, *592*, 267–281. [[CrossRef](#)]
33. Dawson, S.M.; Bowman, M.H.; Leunissen, E.; Sirguyev, P. Inexpensive aerial photogrammetry for studies of whales and large marine animals. *Front. Mar. Sci.* **2017**, *4*, 366. [[CrossRef](#)]
34. Bierlich, K.; Schick, R.; Hewitt, J.; Dale, J.; Goldbogen, J.; Friedlaender, A.; Johnston, D. Bayesian approach for predicting photogrammetric uncertainty in morphometric measurements derived from drones. *Mar. Ecol. Prog. Ser.* **2021**, *673*, 193–210. [[CrossRef](#)]
35. Eurostat. Glossary of Statistical Terms: True Value. Available online: <https://stats.oecd.org/glossary/detail.asp?ID=4557> (accessed on 21 October 2021).
36. Beale, C.S.; Stewart, J.D.; Setyawan, E.; Sianipar, A.B.; Erdmann, M.V. Population dynamics of oceanic manta rays (*Mobula birostris*) in the Raja Ampat Archipelago, West Papua, Indonesia, and the impacts of the El Niño–Southern Oscillation on their movement ecology. *Divers. Distrib.* **2019**, *25*, 1472–1487. [[CrossRef](#)]
37. Setyawan, E.; Erdmann, M.V.; Lewis, S.A.; Mambrasar, R.; Hasan, A.W.; Templeton, S.; Beale, C.S.; Sianipar, A.B.; Shidqi, R.; Heuschkel, H.; et al. Natural history of manta rays in the Bird’s Head Seascape, Indonesia, with an analysis of the demography and spatial ecology of *Mobula alfredi* (Elasmobranchii: Mobulidae). *J. Ocean Sci. Found.* **2020**, *36*, 49–83. [[CrossRef](#)]
38. Setyawan, E.; Erdmann, M.; Gunadharma, N.; Gunawan, T.; Hasan, A.; Izuan, M.; Kasmidi, M.; Lamatenggo, Y.; Lewis, S.; Maulana, N.; et al. A holistic approach to manta ray conservation in the Papuan Bird’s Head Seascape: Resounding success, ongoing challenges. *Mar. Policy* **2022**, *137*, 104953. [[CrossRef](#)]
39. Setyawan, E.; Sianipar, A.B.; Erdmann, M.V.; Fischer, A.M.; Haddy, J.A.; Beale, C.S.; Lewis, S.A.; Mambrasar, R. Site fidelity and movement patterns of reef manta rays (*Mobula alfredi*): Mobulidae using passive acoustic telemetry in northern Raja Ampat, Indonesia. *Nat. Conserv. Res.* **2018**, *3*, 17–31. [[CrossRef](#)]
40. Brown, D.; Christian, W.; Hanson, R.M. Tracker: Video Analysis and Modeling Tool (Version 6.0.1). 2021. Available online: <https://physlets.org/tracker/> (accessed on 1 March 2021).

41. Bolker, B.M.; Brooks, M.E.; Clark, C.J.; Geange, S.W.; Poulsen, J.R.; Stevens, M.H.H.; White, J.-S.S. Generalized linear mixed models: A practical guide for ecology and evolution. *Trends Ecol. Evol.* **2009**, *24*, 127–135. [[CrossRef](#)] [[PubMed](#)]
42. Zuur, A.F.; Ieno, E.N.; Walker, N.J.; Saveliev, A.A.; Smith, G.M. *Mixed Effects Models and Extensions in Ecology with R*; Springer: New York, NY, USA, 2009; Volume 574.
43. Ihaka, R.; Gentleman, R. R: A language for data analysis and graphics. *J. Comput. Graph. Stat.* **1996**, *5*, 299–314. [[CrossRef](#)]
44. Riedel, R.; Caskey, L.M.; Hurlbert, S.H. Length-weight relations and growth rates of dominant fishes of the Salton Sea: Implications for predation by fish-eating birds. *Lake Reserv. Manag.* **2007**, *23*, 528–535. [[CrossRef](#)]
45. Oleksyn, S.; Tosetto, L.; Raoult, V.; Joyce, K.E.; Williamson, J.E. Going batty: The challenges and opportunities of using drones to monitor the behaviour and habitat use of rays. *Drones* **2021**, *5*, 12. [[CrossRef](#)]
46. Butcher, P.A.; Colefax, A.P.; Gorkin, R.A.; Kajiura, S.M.; López, N.A.; Mourier, J.; Purcell, C.R.; Skomal, G.B.; Tucker, J.P.; Walsh, A.J.; et al. The drone revolution of shark science: A review. *Drones* **2021**, *5*, 8. [[CrossRef](#)]
47. Pate, J.H.; Marshall, A.D. Urban manta rays: Potential manta ray nursery habitat along a highly developed Florida coastline. *Endanger. Species Res.* **2020**, *43*, 51–64. [[CrossRef](#)]
48. Oleksyn, S.; Tosetto, L.; Raoult, V.; Williamson, J.E. Drone-based tracking of the fine-scale movement of a coastal stingray (*Bathytoshia brevicaudata*). *Remote Sens.* **2021**, *13*, 40. [[CrossRef](#)]
49. Durban, J.W.; Moore, M.J.; Chiang, G.; Hickmott, L.S.; Bocconcelli, A.; Howes, G.; Bahamonde, P.A.; Perryman, W.L.; LeRoi, D.J. Photogrammetry of blue whales with an unmanned hexacopter. *Mar. Mamm. Sci.* **2016**, *32*, 1510–1515. [[CrossRef](#)]
50. Sabatini, A.M.; Genovese, V. A sensor fusion method for tracking vertical velocity and height based on Inertial and barometric altimeter measurements. *Sensors* **2014**, *14*, 13324–13347. [[CrossRef](#)]
51. Wei, S.; Dan, G.; Chen, H. Altitude data fusion utilising differential measurement and complementary filter. *IET Sci. Meas. Technol.* **2016**, *10*, 874–879. [[CrossRef](#)]
52. Kashiwagi, T. Conservation Biology and Genetics of the Largest Living Rays: Manta Rays. Ph.D. Dissertation, The University of Queensland, Brisbane, Australia, 2014.
53. Kashiwagi, T.; Ito, T.; Sato, F. Occurrences of reef manta ray, *Manta alfredi*, and giant manta ray, *M. birostris*, in Japan, examined by photographic records. *Rep. Jpn. Soc. Elasmobranch Stud.* **2010**, *46*, 20–27.
54. Cortés, E. Life History Patterns and Correlations in Sharks. *Rev. Fish. Sci.* **2000**, *8*, 299–344. [[CrossRef](#)]
55. Hussey, N.E.; Wintner, S.P.; Dudley, S.F.J.; Cliff, G.; Cocks, D.T.; Aaron MacNeil, M. Maternal investment and size-specific reproductive output in carcharhinid sharks. *J. Anim. Ecol.* **2010**, *79*, 184–193. [[CrossRef](#)] [[PubMed](#)]
56. Marshall, A.D.; Pierce, S.J. The use and abuse of photographic identification in sharks and rays. *J. Fish Biol.* **2012**, *80*, 1361–1379. [[CrossRef](#)] [[PubMed](#)]
57. Setyawan, E.; Duffy, C.A.; Erdmann, M.V.; Green, L.; Tindale, S. First insights into the spatial ecology of endangered *Mobula birostris* in Aotearoa. In Proceedings of the New Zealand Marine Sciences Society Conference, Tauranga, New Zealand, 5–8 July 2021.
58. Kristensen, K.; Nielsen, A.; Berg, C.W.; Skaug, H.; Bell, B.M. TMB: Automatic differentiation and Laplace approximation. *J. Stat. Softw.* **2016**, *70*, 21. [[CrossRef](#)]